Applied Radiation and Isotopes 86 (2014) 41–45

Contents lists available at ScienceDirect

Applied Radiation and Isotopes

journal homepage: www.elsevier.com/locate/apradiso

Radiolabeled NGR phage display peptide sequence for tumor targeting

B.L. Faintuch [a,*], E.A. Oliveira [a], R.C. Targino [b], A.M. Moro [b]

[a] Radiopharmacy, Institute of Energy and Nuclear Research, Av. Prof. Lineu Prestes 2242, 05508-000 São Paulo, SP, Brazil
[b] Laboratory of Biopharmacology in Animal Cells, Butantan Institute, Av. Vital Brazil 1500, 05503900 São Paulo, SP, Brazil

HIGHLIGHTS

- Asparagine–glycine–arginine (NGR) peptide is a marker of angiogenesis.
- Radiolabeled NGR was evaluated in different experimental tumor lines.
- Encouraging results were reached with lung and ovarian cancer cells.
- The radiotracer is a candidate for diagnostic application.

ARTICLE INFO

Article history:
Received 28 August 2013
Received in revised form
17 December 2013
Accepted 27 December 2013
Available online 17 January 2014

Keywords:
Cyclic NGR peptide
Radiolabeled
Imaging

ABSTRACT

The asparagine–glycine–arginine (NGR) peptide sequence found by phage display, was radiolabeled with technetium-99*m* and tested in different tumor models. Similar uptake occurred with ovarian and lung tumor cells. Biodistribution of the radiotracer revealed predominant renal excretion with more substantial uptake in animals bearing ovarian tumor cells. In contrast imaging studies indicated better visualization for lung tumor. NGR peptide was characterized as a promising diagnostic candidate, particularly for lung cancer. Improvements are envisaged using NGR combined with RGD as a heterodimer molecule.

1. Introduction

Peptides have been radiolabeled and tested as radiopharmaceuticals for therapy and diagnosis of different diseases. To avoid earlier limitations of peptides as potential clinical tools, new technologies have been developed such as cyclization, antagonist molecules, and phage display technology (Svensen et al., 2012; Thakkar et al., 2013).

Phage display technology conveys peptide sequences interacting with proteins differentially expressed in normal and pathological tissues, including tumor-associated vessels. Peptides selected from phage-display random peptide libraries may target tumor associated receptors with higher affinity and specificity. Among the probes indentified by this technology is the peptide sequence asparagine–glycine–arginine (NGR) (Wang et al., 2012).

Many receptor families can be identified in new tumor vasculature. Two of them are the integrins and aminopeptidase N (CD13), a transmembrane protease. NGR motif attaches to certain integrins along with aminopeptidase N (CD13) (Jiang et al., 2012).

There are reasons to believe that integrins could play a role in the tumor homing properties of NGR-containing ligand through an unusual mechanism, based on deamidation of the asparagine residue and formation of isoaspartate. This reaction converts NGR into *iso*DGR, a novel cell adhesion motif that efficiently binds αvβ3 integrin (Corti et al., 2008).

High expression of CD13 antigen can be detected in a number of human solid tumors, including melanoma (van Hensbergen et al., 2004), prostate, lung and ovarian cancer (Chen et al., 2013). Potential correlations of NGR and CD13 relevant to the present study are depicted in Fig. 1.

The aim of this protocol was evaluation of the pegylated cyclic NGRyk peptide, radiolabeled with ^{99m}Tc (Fig. 2), in tumor cells in vitro and in vivo, as a marker of imaging and angiogenesis in different tumor models. The selected cancer modalities are highly prevalent in humans, and it was hypothesized that clinically relevant findings might arise from such investigation.

2. Materials and methods

2.1. Preparation of the radiotracer

Radiolabeling of the NGR conjugate (MAG_3-PEG_8-c(NGRyk) (piChem Laboratory, Graz, Austria) with ^{99m}Tc, using tartrate

* Corresponding author. Tel.: +551 131 339 531; fax: +551 131 338 956.
E-mail address: blfaintuch@hotmail.com (B.L. Faintuch).

0969-8043/$ - see front matter © 2014 Elsevier Ltd. All rights reserved.
http://dx.doi.org/10.1016/j.apradiso.2013.12.035

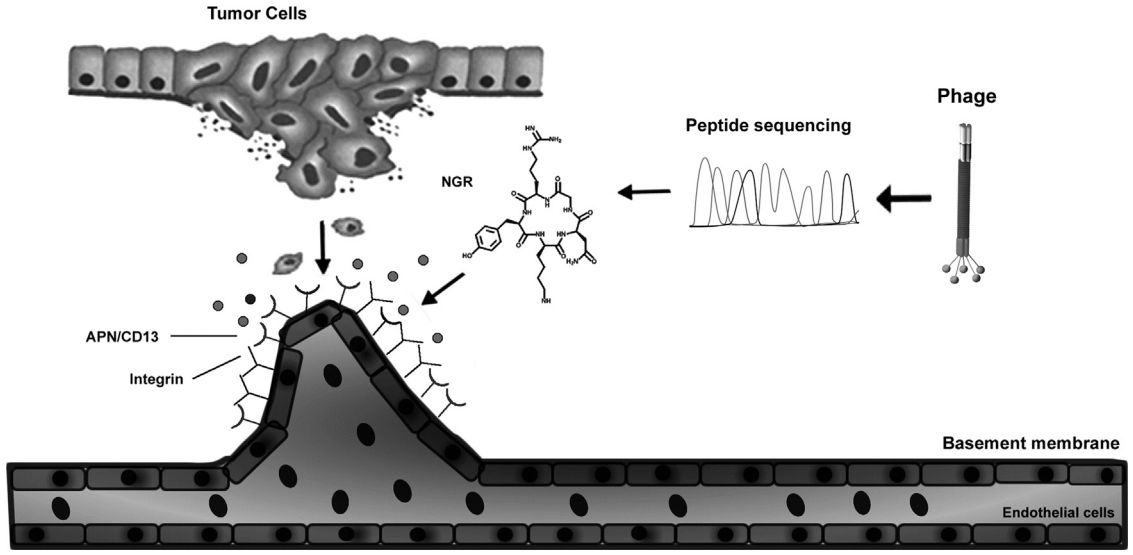

Fig. 1. Correlation between tumor, angiogenesis, phage display, CD13, integrin and NGR.

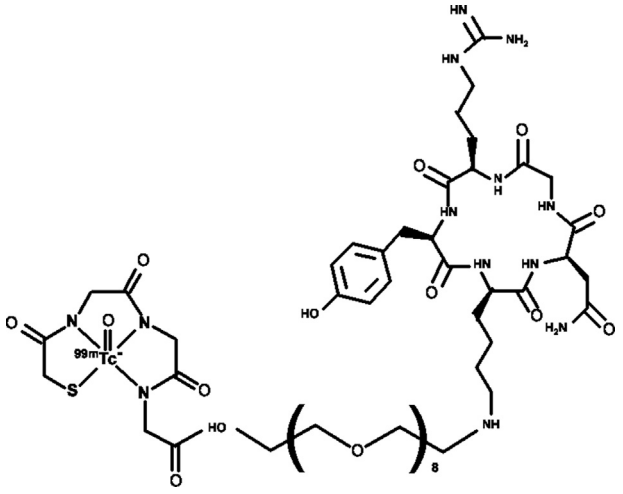

Fig. 2. Structural formula of ^{99m}Tc-MAG$_3$-PEG$_8$-c(NGRyk); chemical formula: $C_{56}H_{92}N_{14}O_{21}S$; molecular weight: 1329.48.

buffer, was previously reported by our group (Oliveira et al., 2012). Briefly, to a vial containing nitrogenated solution of 45 μL of ammonium acetate (0.25 mol/L), 10 μL (7.521 nmol) of MAG$_3$-PEG$_8$-c(NGRyk), 15 mL of tartrate buffer, and 10 μg of stannous chloride in ascorbate–HCl solution (0.1 mol/L), 300 μL of Na^{99m}TcO$_4$ 1850 MBq (50 mCi) from a ^{99}Mo/^{99m}Tc generator (Institute of Energy and Nuclear Research, Sao Paulo, Brazil) was added. Reaction was induced by heating at 100 °C for 20 min. All reagents were purchased from Merck and Sigma-Aldrich (Sao Paulo, Brazil). The radiochemical purity of the complex was assessed by thin-layer chromatography and confirmed by high-performance liquid chromatography (HPLC), using a reverse-phase C18 column, and a flow rate of 1.0 mL/min.

2.2. Tumor cell culture

The cancer cell lines used in this study include human lung carcinoma (A549), androgen-independent human prostate carcinoma (PC-3) and human ovarian carcinoma (OVCAR-3). All cells were originated from American Type Culture Collection (ATCC, USA). PC-3 and OVCAR-3 were grown in RPMI-1640 (Roswell Park Memorial Institute) and A549 in DMEM (Dulbecco's modified Eagles Medium). (Sigma-Aldrich, USA), containing 10 mM HEPES. To ensure growth and viability of the cells, the mediums were supplemented with 10% FBS (Cultilab, Brazil) and gentamicine (Sigma-Aldrich). The cells were kept at 37 °C in a humidified air environment containing 5% CO_2. They were grown to near confluency and were then harvested by trypsinization. Cells (10^6 cells/well) were seeded into six well culture plates for the binding studies 24 h before the experiment. Studies were performed in triplicate ($n=3$). Cells for inoculation in animals were centrifuged (5 min at 100g), counted, and then resuspended in PBS for administration in the animals.

2.3. In vitro cell binding assay

Studies were performed in triplicate at 15, 30, 60, 90, and 120 min time points. Cells were rinsed with assay medium, followed by addition of the assay medium and the radiotracer 90 pM to the cultured wells. For nonspecific binding assays, excess of cold conjugate peptide (1 mmol/L/well) was added. After incubation at 37 °C the cells were rinsed twice with cold PBS. Cell bound radioligand was twice removed by acid wash (50 mmol/L of glycine and 1 mol/L of NaCl, pH=2.8). All phases were collected in measurement tubes for radioactive counting.

2.4. Biodistribution protocol and planar imaging

All experiments were carried out in compliance with the local Animal Welfare Committee. Biodistribution in healthy *Swiss* mice was performed 1 h post injection. Suspensions of tumor cells (5×10^6 in 0.1 mL) were subcutaneously injected into the upper back regions of athymic male nude mice (average weight of 20 g). The tumors were allowed to grow in vivo until a tumor diameter of approximately 1 cm.

^{99m}Tc-conjugated peptide 37 MBq (1 mCi) was injected via the tail vein. Groups of mice ($n=6$) were additionally co-injected with an excess (100 μL, 1 mg/mL) of unlabeled NGR conjugate for receptor blocking. Animals were anesthetized with intraperitoneal injection of urethane solution 15 min before imaging and sacrifice. The animals were sacrified at 60 min postinjection (p.i.) by cervical dislocation. Blood was withdrawn from the heart of the mice. Subsequently major organs, tumor nodule and tissue samples were excised, weighed and counted with a NaI(Tl) gamma counter. Stomach and intestines were emptied before the measurements. The organ and tissue uptake was calculated and expressed as

percentage of injected dose per gram (%ID/g). Imaging was performed in a Planar Gamma Camera (Mediso Imaging System, Budapest, Hungary), employing a low-energy, high-resolution collimator using a $256 \times 256 \times 16$ matrix size with 20% energy window set at 140 keV. Semiquantification of the tumor uptake was evaluated using region-of-interest (ROI) analysis.

2.5. Statistical methods

Numerical results are presented as mean $\pm$ SD, and discrete variables as percentage. Student's *t* test for unpaired data or w2-analysis analysis was used to compare biodistribution and tumor uptake findings, as appropriate. A *p* value of less than 0.05 was considered significant.

3. Results

Radiochemical purity of ^{99m}Tc-MAG$_3$-PEG$_8$-c(NGRyk) was calculated by RP-HPLC, and corresponded to 99.3 $\pm$ 0.4%, using the gradient systems consisting of 0.1% trifluoroacetic acid/water (solvent A) and 0.1% trifluoroacetic acid/acetonitrile (solvent B). No free pertechnetate impurity was observed in the radiochromatogram (Fig. 3). The retention time (t_R) for ^{99m}TcO$_4$ was 4 min, and for the radiotracer the value was 10.69 min. The specific activity was 245.98 MBq/nmoles (6.64 mCi/nmole).

In vitro studies (Fig. 4) with lung tumor cells achieved the highest binding profile, at 5 and 30 min compared to the other cells ($p=0.02$), but with 1 h of incubation, similar binding for ovarian and lung tumor cells occurred ($p > 0.05$). Prostate tumor cells PC-3 exhibited the lowest binding affinity at all studied times ($p=0.04$). In blocking assays with excess of the cold peptide conjugate, 11.0% of the lung A549 cells and 28.7% of ovarian OVCAR-3 were blocked after 2 h of incubation.

The results of the biodistribution studies of ^{99m}Tc-MAG$_3$-PEG$_8$-c(NGRyk) in athymic mice with subcutaneous tumor cells at 1 h p.i. are summarized in Table 1.

Values are expressed as %ID/g (for blood %ID/mL). The biodistribution revealed predominant renal excretion, blood uptake in the range of 0.5 ID/mL, and uptake in most organs and tissues below 1% ID/g.

The 1 h time adopted for biodistribution and imaging was based on blood clearance of the radiotracer in a previous study using healthy *Swiss* mice (Oliveira et al., 2012).

Tumor uptake *in-vivo* was more pronounced in animals bearing ovarian tumor cells. The co-administration of an excess amount of unlabeled RGD decreased the uptake of ^{99m}Tc-MAG$_3$-PEG$_8$-c(NGRyk) in the tumor, which was 62% blocked ($p < 0.05$) (Fig. 5). Better visualization was documented for lung tumor, with ROI value of 2.65% (Fig. 6). The tumor/muscle ratio for animals bearing lung tumor cells (A549) was 3.25 and for ovarian tumor cells (OVCAR-3) it was 2.77.

4. Discussion

Prostate and lung cancer are among the most frequent and disease burden did not abate even after introduction of PSA testing and decline of smoking in males (Berg, 2011). Ovarian cancer is the leading cause of death from gynecological malignancies. Ovarian cancer generally presents in advanced stages with a high case/fatality ratio, however survival is more favorable if diagnosed earlier. Nevertheless, there is a dearth of approved markers for early detection (Cramer et al., 2011).

Angiogenic blood vessels express markers that are either present at very low levels or are entirely absent in normal blood vessels. So there is an advantage to use radiotracers specific to solid tumor angiogenesis (Pasqualini et al., 2000).

Design of the molecule, choice of chelator as well as spacer for peptide conjugation may all be important, as they are related to improved pharmacokinetics of the radiotracer.

Pegylation shields peptides from enzymatic degradation and thus reduces proteolysis, also enhancing overall hydrophilicity of the compound (Däpp et al., 2011). In such circumstances one may observe increased peptide half-life and stability, along with reduced immunogenicity (Sanli et al., 2005).

The most used bifunctional technetium chelators are 6-hydrazinonicotinic acid (HYNIC) and mercaptoacetylglycylglycylglycylglycine (MAG$_3$). The former captures technetium at extremely low concentrations, yet the structure of the labeled complexes tends to be heterogeneous and incompletely characterized (Banerjee et al., 2005).

As alluded to before cyclic peptides, in contrast to linear ones, are more resistant to both exo- and endoproteases. Synthesis may conducted using cysteine for the formation of a disulfide bridge (White and Yudin, 2011). In our study we used for cyclization the lysine residue, conjugated to polyethylene glycol (PEG$_8$) and MAG$_3$ as bifunctional chelator.

NGR radiolabeled with ^{99m}Tc has already been investigated by our group (Oliveira et al., 2012). The high radiochemical purity of the radiotracer (> 98%) stimulated further analysis encompassing

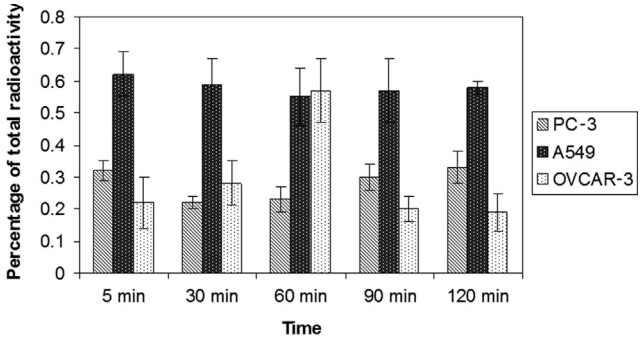

Fig. 4. Uptake binding in tumor cells ($n=3$).

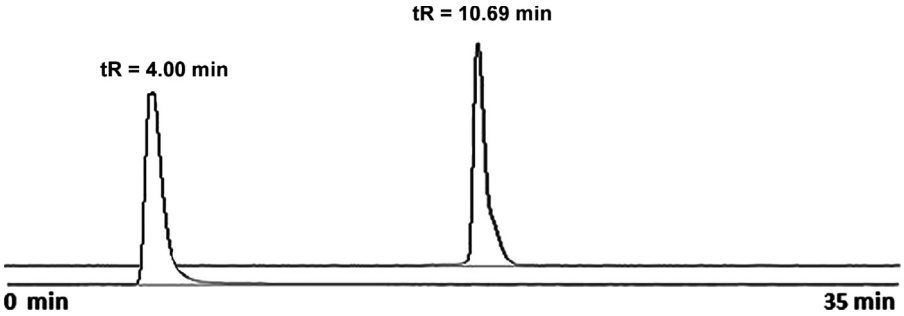

Fig. 3. HPLC radiochromatograms—^{99m}TcO$_4$ tR = 4.00 min; ^{99m}Tc-MAG$_3$-PEG$_8$-c(NGRyk)—tR = 10.69 min.

Table 1
Biodistribution of ^{99m}Tc-MAG$_3$-PEG$_8$-c(NGRyk), in healthy Swiss mice and in Nude mice bearing tumor cells, (%ID/g), 1 h after injection.

	Healthy	PC-3		A549		OVCAR-3	
		w/Block	Block	w/Block	Block	w/Block	Block
Blood	0.83 ± 0.53	0.22 ± 0.08	0.31 ± 0.15	0.40 ± 0.19	0.65 ± 0.21	0.63 ± 0.07	0.94 ± 0.13
Heart	0.55 ± 0.41	0.21 ± 0.11	0.26 ± 0.13	0.28 ± 0.06	0.16 ± 0.08	0.46 ± 0.21	0.50 ± 0.27
Lungs	1.40 ± 0.91	0.62 ± 0.18	1.01 ± 0.92	0.85 ± 0.27	0.46 ± 0.02	1.27 ± 0.49	1.17 ± 0.55
Kidneys	2.61 ± 1.02	2.36 ± 0.45	2.18 ± 0.88	3.40 ± 0.84	1.11 ± 0.16	4.85 ± 2.15	4.38 ± 1.50
Spleen	0.43 ± 0.21	0.23 ± 0.10	0.20 ± 0.06	0.21 ± 0.11	0.17 ± 0.11	0.50 ± 0.20	0.38 ± 0.19
Stomach	0.57 ± 0.37	0.43 ± 0.10	0.25 ± 0.01	0.62 ± 0.25	0.31 ± 0.12	0.77 ± 0.31	0.69 ± 0.30
Pancreas	0.32 ± 0.21	0.32 ± 0.16	0.37 ± 0.12	0.35 ± 0.04	0.60 ± 0.14	0.50 ± 0.27	0.39 ± 0.22
Liver	1.49 ± 0.80	0.33 ± 0.12	0.24 ± 0.01	0.71 ± 0.27	0.28 ± 0.02	0.84 ± 0.21	0.74 ± 0.34
Large intestine	0.57 ± 0.34	0.55 ± 0.28	0.49 ± 0.15	0.63 ± 0.25	0.59 ± 0.15	1.13 ± 0.53	0.55 ± 0.23
Small intestine	1.74 ± 0.90	0.76 ± 0.14	0.41 ± 0.04	2.23 ± 0.41	1.36 ± 0.50	2.06 ± 0.78	1.95 ± 0.99
Muscle	0.29 ± 0.14	0.24 ± 0.08	0.10 ± 0.04	0.20 ± 0.06	0.18 ± 0.05	0.35 ± 0.17	0.33 ± 0.28
Bone	0.42 ± 0.24	0.84 ± 0.32	0.96 ± 0.26	0.68 ± 0.21	0.70 ± 0.33	1.01 ± 0.36	0.30 ± 0.21
Tumor		0.36 ± 0.11	0.32 ± 0.10	0.65 ± 0.14	0.26 ± 0.06	0.97 ± 0.38	0.37 ± 0.05

Abbreviations: Block: Receptor blocking; w/Block: Without receptor blocking; Mean ± SD (n=6).

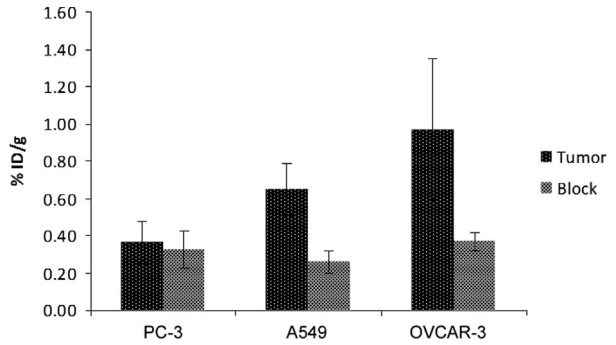

Fig. 5. Uptake of radiotracer in tumor and blocked tumor, 1 h after injection.

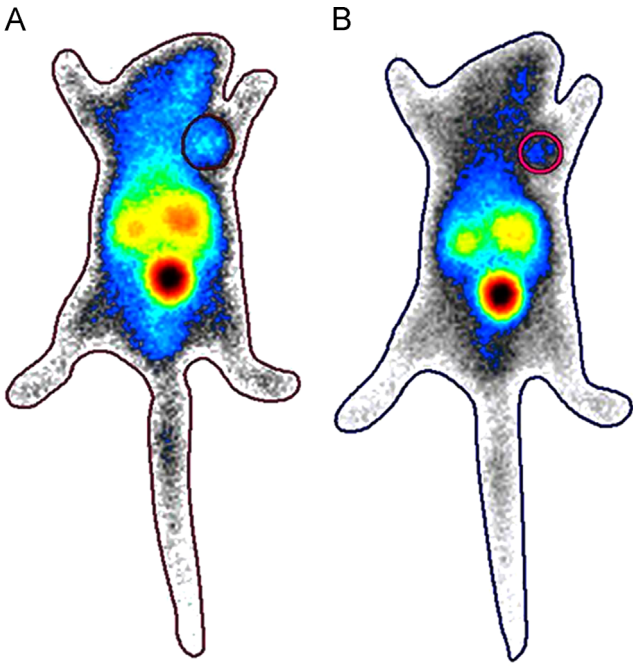

Fig. 6. Scintigraphic image in urethane-anesthetized nude mice of (A) lung tumor and (B) ovarian tumor (0.1 mL/37 MBq).

in vitro and *in vivo* evaluation, without the time consuming steps of purification and drying of the compound.

In the current study, we evaluated the uptake of the radiotracer ^{99m}Tc-MAG$_3$-PEG$_8$-c(NGRyk) in three different tumor cells namely lung (A549), prostate (PC-3) and ovarian (OVCAR-3), differently from the initial protocol addressing melanoma (Oliveira et al., 2012).

NGR sequence can bind to new vasculature via two types of receptors: aminopeptidase N (CD13), a cell-surface tumor target, and integrin $\alpha_v\beta_3$, although binding mechanisms are different. CD13 receptor mediates NGR binding to tumor vasculature, but not to other CD13 rich tissues (Chen et al., 2013; Wei et al., 2013). *In vivo* evaluation was performed using the time point of 1 h post injection. Good blood clearance was noticed, favoring the utilization of imaging techniques.

Cancer cell surface-binding ligands were searched by combinatorial chemistry technology and not phage display by Aina et al., (2005), confirming the binding specificity of the NGR sequence in cancer cell lines. They reported that ovarian tumor cells (OVCAR-3) were endowed with very strong binding (> 30 cells per bead), prostate (PC-3) with strong binding (20–30 cells per bead), and lung cells (A549) with moderate binding (10–20 cells per bead). Several other reports have demonstrated the ability of NGR peptides to specifically target tumor vasculature in vivo (Krumpe and Mori, 2007).

Approximately 90% of primary ovarian cancers are epithelial tumors (Boger-Megiddo and Weiss, 2005), and epithelial tissues often undergo more robust angiogenesis.

Zhou et al., (2011), reported the total integrin expression levels of some tumor cells, two of them used in our study. They found that lung cells A549 had higher expression of integrin $\alpha_v\beta_3$ than prostate cells PC-3. The same proportions correspond to our results, both in *in vitro* assays and during tumor uptake *in vivo*. Fig. 4 shows that the profile of cells A549 in different times was high and stable. As reported by Wei et al., (2013), A549 cells don't express CD13 on the membranes so uptake is only due integrin.

A few groups have performed assays with radiolabeled NGR in a variety of tumor cell strains such as Lewis mouse lung carcinoma (LLC), human colorectal adenocarcinoma (Colo 205) (Jiang et al., 2012), human fibrosarcoma HT-1080 (Chen et al., 2013) and HepG2 hepatoma (Ma et al., 2013). The two last articles evaluated both NGR monomer and dimer. Tumor uptake in these experiences was remarkable specially when dimers of the peptide were focused, nevertheless uptake in main organs namely liver, stomach and intestine was very substantial also, even after 4 h, representing a drawback. The explanation could be design of the NGR molecule surrounded by glycine and cysteine.

It's worth emphasizing that in this model radioactivity in the liver and gastrointestinal tract remained moderate, unlikely to interfere with detection of tumor and metastases in the abdominal area. Excretion was mainly renal and fast blood depuration was another favorable feature.

5. Conclusion

A novel molecule for tumor diagnosis was designed and evaluated. Promising results were reached with lung and ovarian cancer cells. The results can potentially be enhanced by the improvements in radiotracer design, such as using a homodimer $(NGR)_2$ or heterodimer (RGD-NGR), for CD13 and integrin expression in different tumors.

Acknowledgements

The authors thank Jose Coelho de Oliveira Junior for help during biological experiments, to Natanael Gomes da Silva for imaging technical support and Maria Neide Ferreira Mascarenhas for assistance with animal facilities.

References

Aina, O.H., Marik, J., Liu, R., Lau, D.H., Lam, K.S., 2005. Identification of novel targeting peptides for human ovarian cancer cells using "one-bead one-compound"combinatorial libraries. Mol. Cancer Ther. 4, 806–813.

Banerjee, S.R., Maresca, K.P., Francesconi, L., Valliant, J., Babich, J.W., Zubieta, J., 2005. New directions in the coordination chemistry of ^{99m}Tc: a reflection on technetium core structures and a strategy for new chelate design. Nucl. Med. Biol. 32 (1), 1–20.

Berg, C.D., 2011. The prostate, lung, colorectal and ovarian cancer screening trial: the prostate cancer screening results in context. Acta Oncol 50 (1), 12–17.

Boger-Megiddo, I., Weiss, N.S., 2005. Histologic subtypes and laterality of primary ovarian tumors. Gynecol. Oncol. 97, 80–83.

Chen, K., Ma, W., Li, G., Wang, J., Yang, W., Yap, L.P., Hughes, L.D., Park, R., Conti, P.S., 2013. Synthesis and evaluation of 64Cu-labeled monomeric and dimeric NGR peptides for MicroPET imaging of CD13 receptor expression. Mol. Pharm. 10 (1), 417–427.

Corti, A., Curnis, F., Arap, W., Pasqualini, R., 2008. The neovasculature homing motif NGR: more than meets the eye. Blood 112 (7), 2628–2635.

Cramer, D.W., Bast , R.C., Berg, C.D., Diamandis, E.P., Godwin, A.K., Hartge, P., Lokshin, A.E., Lu, K.H., McIntosh, M.W., Mor, G., Patriotis, C., Pinsky, P.F., Thornquist, M.D., Scholler, N., Skates, S.J., Sluss, P.M., Srivastava, S., Ward, D.C., Zhang, Z., Zhu, C.S., Urban, N., 2011. Ovarian cancer biomarker performance in prostate, lung, colorectal, and ovarian cancer screening trial specimens. Cancer Prev. Res. (Phila.) 4 (3), 365–374.

Däpp, S., García-Garayoa, E., Maes, V., Brans, L., Tourwé, D.A., Müller, C., Schibli, R., 2011. Pegylation of ^{99m}Tc-labeled bombesin analogues improves their pharmacokinetic properties. Nucl. Med. Biol. 38 (7), 997–1009.

Jiang, W., Jin, G., Ma, D., Wang, F., Fu, T., Chen, X., Chen, X., Jia, K., Marikar, F.M., Hua, Z., 2012. Modification of cyclic NGR tumor neovasculature homing motif sequence to human plasminogen kringle 5 improves inhibition of tumor growth. PLoS One 7 (5), e37132.

Krumpe, L.R.H., Mori, T., 2007. Potential of phage-displayed peptide library technology to identify functional targeting peptides. Expert Opin. Drug Discovery 2 (4), 525.

Ma, W., Kang, F., Wang, Z., Yang, W., Li, G., Ma, X., Li, G., Chen, K., Zhang, Y., Wang, J., 2013. (99m)Tc-labeled monomeric and dimeric NGR peptides for SPECT imaging of CD13 receptor in tumor-bearing mice. Amino Acids 44 (5), 1337–1345.

Oliveira, E.A., Faintuch, B.L., Núñez, E.G., Moro, A.M., Nanda, P.K., Smith, C.J., 2012. Radiotracers for different angiogenesis receptors in a melanoma model. Melanoma Res. 22 (1), 45–53.

Pasqualini, R., Koivunen, E., Kain, R., Lahdenranta, J., Sakamoto, M., Stryhn, A., Ashmun, R.A., Shapiro, L.H., Arap, W., Ruoslahti, E., 2000. Aminopeptidase N is a receptor for tumor-homing peptides and a target for inhibiting angiogenesis. Cancer Res. 60 (3), 722–727.

Sanli, K.N., Mcguire, M.J., Newgard, C.B., Johnston, S.A., Brown, K.C., 2005. Peptide-mediated targeting of the islets of Langerhans. Diabetes 54 (7), 2103–2108.

Svensen, N., Walton, J.G.A., Bradley, M., 2012. Peptides for cell-selective drug delivery. Trends Pharmacol. Sci. 33 (4), 186–192.

Thakkar, A., Trinh, T.B., Pei, D., 2013. Global analysis of peptide cyclization efficiency. ACS Comb. Sci. 15 (2), 120–129.

van Hensbergen, Y., Broxterman, H.J., Rana, S., Van Diest, P.J., Duyndam, M.C., Hoekman, K., Pinedo, H.M., Boven, E., 2004. Reduced growth, increased vascular area, and reduced response to cisplatin in CD13-overexpressing human ovarian cancer xenografts. Clin. Cancer Res. 10, 1180–1191.

Wang, R.E., Niu, Y., Wu, H., Hu, Y., Cai, J., 2012. Development of NGR-based anticancer agents for targeted therapeutics and imaging. Anticancer Agents Med. Chem. 12, 76–86.

Wei, Y., Yin, G., Yin, H., Yan, D., Ma, C., Huang, Z., Liao, X., Yao, Y., Chen, X., 2013. Inhibiting effects of a cyclic peptide CNGRC on proliferation and migration of tumor cells in vitro. Int. J. Pept. Res. Ther. 19, 163–173.

White, C.J., Yudin, A.K, 2011. Contemporary strategies for peptide. Nat. Chem. 3, 509–524.

Zhou, Y., Kim, Y.S., Chakraborty, S., Shi, J., Gao, H., Liu, S, 2011. ^{99m}Tc-labeled cyclic RGD peptides for noninvasive monitoring of tumor integrin $\alpha V\beta 3$ expression. Mol. Imaging 10 (5), 386–397.